JETIR.ORG ISSN: 2349-5162 | ESTD Year : 2014 | Monthly Issue
JOURNAL OF EMERGING TECHNOLOGIES AND INNOVATIVE RESEARCH (JETIR)
An International Scholarly Open Access, Peer-reviewed, Refereed Journal

Hemodynamic Characterization of Tapered Arterial Stenosis with Dilatation Using Ellis Fluid Biorheology

[1]Manmohan Singh,[2]R.K. Shrivastav
[1]Research Scholar, [2]Professor
[1-2]Department of Mathematics, Agra College, Agra, Uttar Pradesh (India),
Affiliated to Dr. Bhimrao Ambedkar University, Agra, Uttar Pradesh (India)

Abstract: One of the most prevalent symptoms of cardiovascular disease, which remains a major global health concern, is arterial stenosis. In order to effectively diagnose and treat tapering arterial stenosis with dilatation, it is essential to understand the hemodynamic changes that occur. In order to thoroughly evaluate the fluid dynamics in these vascular situations, this work takes a complex approach by using the Ellis fluid biorheology model. A complex geometric structure seen in numerous vascular diseases is the tapering arterial stenosis with dilatation. Using computational fluid dynamics (CFD) models, the research aims to clarify the complex relationship between fluid rheology and vascular shape. In contrast to more conventional Newtonian models, the Ellis fluid model more accurately depicts blood rheology by taking into account the non-Newtonian behavior and shear-thinning characteristics of blood. This research takes a methodical look at how hemodynamic factors such wall shear stress, velocity profiles, resistance to flow, and volumetric flow rate are affected by different levels of yield stress, shape parameter, and viscosity coefficient. The results show how important it is to take non-Newtonian factors into consideration when trying to foretell the hemodynamic effects of tapering arterial stenosis with dilatation. In addition, the study delves into the possible clinical consequences of these hemodynamic changes, with the goal of enhancing our knowledge of disease development and directing tailored treatment approaches. This research highlights the significance of including realistic biorheological factors in a thorough understanding of vascular pathophysiology and provides valuable insights into the hemodynamics of tapered arterial stenosis with dilatation by combining advanced computational models with clinically relevant geometric variations. These findings have the potential to lead to better methods of diagnosis and more efficient treatments for cardiovascular illnesses.

Keywords: Arterial stenosis, Dilatation, Hemodynamic parameters, Ellis fluid model, Shear stress, Pressure drop

I. INTRODUCTION

Research in the intricate and multidisciplinary field of hemodynamic evaluation of tapered arterial stenosis with dilatation utilizing Ellis fluid biorheology integrates concepts from biomedical engineering, rheology, and fluid mechanics. Using Ellis fluid models, this area investigates the hemodynamic behavior and its effects on vascular health as it pertains to blood flow through arteries with particular geometric features as tapering stenosis and dilatation.The buildup of atherosclerotic plaques and other pathophysiological processes can lead to arterial stenosis, which is the narrowing of an artery. When the diameter of an artery gradually decreases, a condition known as tapered stenosis occurs, making blood flow more difficult. In contrast, dilatation entails expanding a vessel, which can have intricate effects on hemodynamics as well. In this regard, the decision to use Ellis fluid models is crucial. The shear-thinning characteristic of Ellis fluids, which are non-Newtonian fluids, indicates that their viscosity reduces as the shear rate increases. Compared to more conventional Newtonian models, this rheological feature better captures how blood behaves. In order to more accurately portray the physiological conditions, hemodynamic characterisation utilizing Ellis

fluid biorheology accounts for the non-uniform nature of blood flow in tapering stenotic and dilated arteries. Evaluation of velocity profiles, pressure distribution, wall shear stress, and other pertinent parameters within the artery geometry may be important components of the hemodynamic characterization. Blood flow patterns under different situations are frequently simulated using computational fluid dynamics (CFD) and mathematical modeling. If we want to know how these geometric differences affect vascular health, we need to know how Ellis fluid biorheology explains the hemodynamic features of tapering arterial stenosis with dilatation. In the long run, this study might help us control and avoid problems caused by vascular anomalies by paving the way for better diagnostic and treatment methods for cardiovascular disorders. Models of blood flow that are not Newtonian were developed by Chaturani et al. (1985). Their focus is on how the narrowing affects blood flow within the artery. In order to delve into the stenosis vessel investigation, several mathematical fluid models are created, taking into account non-Newtonian properties. Utilizing the limited distinction strategy (FDM) and taking into account blood as a non-Newtonian liquid, Chakravarty and Mandal (1994) registered the time-subordinate blood stream in a covering stenotic corridor. In their numerical model of blood vessel blood stream, Mandal and Chakravarty (2000) expected the blood to be a Newtonian liquid and utilized the clinically pertinent time-differing design of covering stenosis shows in the supply route lumen and vascular wall adaptable deformability. The one-layered Bingham plastic progression of blood through a small conduit with a few stenoses and post-stenotic dilatation was tended to by Singh and Singh (2012). They calculated the resistance-to-flow ratio for yield stresses of 0,.02 and.04 n/m2 using blood viscosities of 0.00345, 0.004, and 0.00455 Pa.s and fluxes of 1, 10, and 100, respectively. Prasad et al. (2014) investigated the possibility of a constant flow of Jeffrey fluid through a tube with both dilatations and constrictions. Expecting a mid-line stenosis, they decided the accompanying conditions for speed, pressure drop, volumetric stream rate, protection from stream, and wall shear pressure: Rf is the ratio of the height of the stenosis to the post-stenotic dilatation. Blood stream through a tightening corridor with stenosis and dilatation was concentrated by Priyadharshini and Ponalagusamy (2015) utilizing the incompressible Herschel-Bulkley liquid model. Wall shear pressure and stream obstruction both ascent forcefully with expanding pivotal distance, and the ascent is considerably more articulated in the circumstance of a combining tightening corridor, as per their perceptions. Through a pivotally even, laminar, steady, one-layered blood stream in the corridor, Oghre and Okoronkwo (2016) concentrated on the effect of multi-unpredictable molded stenoses on non-Newtonian liquid. According to the Bingham plastic fluid equation, blood can flow above the yield stress value but cannot flow below it because it is a non Newtonian fluid. In a round tube with stenosis and dilatations, Prasad et al. (2016) concentrated on the progression of incompressible pair pressure liquid. There was a slight axially symmetric stenosis, according to their assumptions. The conditions for stream, speed, pressure drop, and wall shear pressure were additionally created in the wake of linearizing the stream conditions. Stream obstruction and strain drop both ascent with stenosis level however fall with post-stenotic dilatation, as per their discoveries. In 2016, Maiti explored the completely developed one-layered non-Newtonian blood move through a vein tube with post-stenotic dilatation and different stenoses. A pivotally symmetric yet radially non-symmetric numerous stenosed corridor was proposed for the consistent progression of blood. The impact of slip on consistent Herschel-Bulkley liquid course through a stenosed cylinder and its post-stenosis dilatation was concentrated by Raja et al. (2018). The stenosis is probably not too bad. Logical recipes for stream obstruction, speed, pressure drop, and wall shear pressure have been inferred. New to this study is Hussain et al. (2023) thought of computationally temperamental blood stream in a course with symmetric stenosis and aneurysm. Their examination can possibly propel clinical information by working on the recognition of stenotic-aneurysmal ailments and growing comprehension we might interpret the stenotic-aneurysmal conduit.

II. MATHEMATICAL FORMULATION AND SOLUTION

A condition that depicts the calculation of a wall can be composed as follows:

$$\frac{R}{R_0} = \begin{bmatrix} 1 - B_i\left[l_i^{s_i-1}(z-\alpha_i) - (z-\alpha_i)^{s_i}\right] & \alpha_i \le z \le \beta_i \\ 1 & Otherwise \end{bmatrix} \quad (1)$$

The shape of thei^{th} stenosis is determined by the parameter $(s_i \geq 2)$, which is related to the arterial radius R, the normal radius R_0, and the length of the i^{th}stenosis is l_i.

The distance from the beginning of the segment to the beginning of the i^{th} stenosis, denoted as α_i, is provided by

$$\alpha_i = \sum_{j=1}^{j}(d_j + l_j) - l_i \quad (2)$$

The distance between the start of the section and the finish of the i^{th} stenosis, meant as, still up in the air by

$$\beta_i = \sum_{j=1}^{i}(d_j + l_j) \quad (3)$$

The starting point of the i^{th} stenosis is separated from the previous stenosis's end or, in the case where $i = 1$, from the segment's beginning by the distance d_i.

This is where the value of the constant B_i is determined by

$$B_i = \frac{\delta_i}{R_0 l_i^{s_i}} \frac{s_i^{\frac{s_i}{s_i-1}}}{s_i-1} \quad (4)$$

The Ellis fluid model's constitutive equation is given by:

$$\tau = \tau_0 + K\dot{\gamma}^n + \eta\dot{\gamma} \quad (5)$$

Here's a breakdown of the terms:

τ: Shear stress.

τ_0: Yield pressure, the base pressure expected to start stream.

K: Consistency index, a measure of the fluid's resistance to deformation.

$\dot{\gamma}$: Shear rate.

n: Flow behavior index, influencing the degree of shear-thinning or shear-thickening behavior.

η: Viscosity coefficient, representing the viscosity of the fluid.

The value of n can shift, and it decides the level of shear-diminishing or shear-thickening conduct in the liquid:

$n < 1$: Shear-diminishing way of behaving (diminishing thickness with expanding shear rate).

$n = 1$: Newtonian way of behaving (steady consistency paying little heed to shear rate).

$n > 1$: Shear-thickening way of behaving (expanding consistency with expanding shear rate).

Here we consider the case $n = 1$

$$\tau = \tau_0 + K\dot{\gamma} + \eta\dot{\gamma}$$

$$\tau = \tau_0 + (K + \eta)\dot{\gamma}$$

$$f(\tau) = \dot{\gamma} = -\frac{du}{dr} = \frac{\tau-\tau_0}{K+\eta} \quad (6)$$

The flux Q that happens through the artery is determined by

$$Q = \int_0^R 2\pi r u \, dr \quad (7)$$

Solving equation (7) and using the no-slip boundary condition $u = 0$ when $r = R$, we get

$$Q = \int_0^R 2\pi r u \, dr = 2\pi \left[\left(\frac{r^2}{2}u\right)_0^R - \int_0^R \frac{du}{dr}\frac{r^2}{2}dr\right] = \pi \int_0^R r^2 \left(-\frac{du}{dr}\right) dr$$

$$Q = \pi \int_0^R r^2 \left(-\frac{du}{dr}\right) dr \quad (8)$$

Applying (6) in (8) to obtain

$$Q = \pi \int_0^R r^2 f(\tau)\ dr \tag{9}$$

It is possible to obtain the formulae for τ and τ_R, which represent the shear at the wall, or when r equals R.

$$\tau = -\frac{r}{2}\frac{dp}{dz}, \tau_R = -\frac{R}{2}\frac{dp}{dz} \tag{10}$$

Here, p represents the pressure. As a result of equations (8) and (9), we obtain

$$\frac{\tau}{\tau_R} = \frac{r}{R} \Rightarrow r = \frac{R}{\tau_R}\tau \Rightarrow dr = \frac{R}{\tau_R}d\tau$$

$$Q = \pi \int_0^R r^2 f(\tau)\ dr = \pi \int_0^{\tau_R} \left(\frac{R}{\tau_R}\tau\right)^2 f(\tau)\ \frac{R}{\tau_R}d\tau = \pi \int_0^{\tau_R} \left(\frac{R}{\tau_R}\tau\right)^2 f(\tau)\ \frac{R}{\tau_R}d\tau$$

$$= \pi \frac{R^3}{{\tau_R}^3} \int_0^{\tau_R} \tau^2 f(\tau)\ d\tau \tag{11}$$

The result can be obtained by substituting equation (6) and reconfiguring the equation.

$$Q = \pi \frac{R^3}{{\tau_R}^3} \int_0^{\tau_R} \tau^2 \frac{\tau - \tau_0}{K+\eta} d\tau = \frac{\pi R^3}{(K+\eta){\tau_R}^3} \int_0^{\tau_R} (\tau^3 - \tau^2\tau_0)\ d\tau = \frac{\pi R^3}{(K+\eta){\tau_R}^3} \left[\frac{\tau^4}{4} - \frac{\tau^3}{3}\tau_0\right]_0^{\tau_R}$$

$$Q = \frac{\pi R^3}{(K+\eta){\tau_R}^3}\left(\frac{{\tau_R}^4}{4} - \frac{{\tau_R}^3}{3}\tau_0\right) = \frac{\pi R^3 {\tau_R}^3}{(K+\eta){\tau_R}^3}\left(\frac{\tau_R}{4} - \frac{\tau_0}{3}\right) = \frac{\pi R^3}{(K+\eta)}\left(\frac{\tau_R}{4} - \frac{\tau_0}{3}\right)$$

$$\left(\frac{\tau_R}{4} - \frac{\tau_0}{3}\right) = \frac{Q(K+\eta)}{\pi R^3} \Rightarrow \frac{\tau_R}{4} = \frac{Q(K+\eta)}{\pi R^3} + \frac{\tau_0}{3} \Rightarrow \tau_R = \frac{4Q(K+\eta)}{\pi R^3} + \frac{4\tau_0}{3}$$

$$Q = \frac{\pi R^3}{(K+\eta)}\left(\frac{\tau_R}{4} - \frac{\tau_0}{3}\right) \tag{12}$$

From equation (11), we get

$$\tau_R = \frac{4Q(K+\eta)}{\pi R^3} + \frac{4\tau_0}{3} \tag{13}$$

Putting the values of τ_R from equation (9) into the equation (12), we get

$$-\frac{R}{2}\frac{dp}{dz} = \frac{4Q(K+\eta)}{\pi R^3} + \frac{4\tau_0}{3}$$

$$\frac{dp}{dz} = -\frac{2}{R}\left[\frac{4Q(K+\eta)}{\pi R^3} + \frac{4\tau_0}{3}\right] \tag{14}$$

Equation (12) is integrated with respect to z, with the condition that p equals p_0 when z equals zero and p equals p_1 when z equals l.

$$p_1 - p_0 = -\frac{8Q(K+\eta)}{\pi}\int_0^l \frac{1}{R^4}dz - \frac{8\tau_0}{3}\int_0^l \frac{1}{R}dz$$

$$\lambda = \frac{p_1-p_0}{Q} = -\frac{8(K+\eta)}{\pi R_0^4}\int_0^l \left(\frac{R}{R_0}\right)^{-4} dz - \frac{8\tau_0}{3R_0Q}\int_0^l \left(\frac{R}{R_0}\right)^{-1} dz$$

$$g_1 = \frac{8(K+\eta)}{\pi R_0^4}, g_2 = \frac{8\tau_0}{3R_0Q}$$

$$\lambda = \frac{p_1-p_0}{Q} = -g_1\int_0^l \left(\frac{R}{R_0}\right)^{-4} dz - g_2\int_0^l \left(\frac{R}{R_0}\right)^{-1} dz$$

$$\lambda = \frac{p_1-p_0}{Q} = -g_1\left[\int_0^{\alpha_j} dz + \sum_{j=1}^{m}\int_{\alpha_j}^{\beta_j}\left(\frac{R}{R_0}\right)^{-4} dz + \sum_{j=1}^{m-1}\int_{\beta_j}^{\alpha_{j+1}} dz + \int_{\beta_k}^{l} dz\right] - g_2\left[\int_0^{\alpha_j} dz + \sum_{j=1}^{m}\int_{\alpha_j}^{\beta_j}\left(\frac{R}{R_0}\right)^{-1} dz + \sum_{j=1}^{m-1}\int_{\beta_j}^{\alpha_{j+1}} dz + \int_{\beta_k}^{l} dz\right]$$

$$\lambda = \frac{p_1-p_0}{Q} = -g_1\left[\int_0^{\alpha_j} dz + \sum_{j=1}^{m}\int_{\alpha_j}^{\beta_j}\left(\frac{R}{R_0}\right)^{-4} dz + \sum_{j=1}^{m-1}\int_{\beta_j}^{\alpha_{j+1}} dz + \int_{\beta_k}^{l} dz\right] - g_2\left[\int_0^{\alpha_j} dz + \sum_{j=1}^{m}\int_{\alpha_j}^{\beta_j}\left(\frac{R}{R_0}\right)^{-1} dz + \sum_{j=1}^{m-1}\int_{\beta_j}^{\alpha_{j+1}} dz + \int_{\beta_k}^{l} dz\right]$$

$$\lambda = \frac{p_1-p_0}{Q} = -g_1\left[\int_0^{\alpha_j} dz + \sum_{j=1}^{m}\int_{\alpha_j}^{\beta_j}\left(\frac{R}{R_0}\right)^{-4} dz + \sum_{j=1}^{m-1}\int_{\beta_j}^{\alpha_{j+1}} dz + \int_{\beta_k}^{l} dz\right] - g_2\left[\int_0^{\alpha_j} dz + \sum_{j=1}^{m}\int_{\alpha_j}^{\beta_j}\left(\frac{R}{R_0}\right)^{-1} dz + \sum_{j=1}^{m-1}\int_{\beta_j}^{\alpha_{j+1}} dz + \int_{\beta_k}^{l} dz\right]$$

$$\lambda = -g_1\left[\sum_{j=1}^{m+1} d_j + I_1\right] - g_2\left[\sum_{j=1}^{m+1} d_j + I_2\right]$$

$$I_1 = \sum_{j=1}^{m+1}\int_{\alpha_j}^{\beta_j}\left(\frac{R}{R_0}\right)^{-4} dz, I_2 = \sum_{j=1}^{m+1}\int_{\alpha_j}^{\beta_j}\left(\frac{R}{R_0}\right)^{-1} dz$$

$$\lambda = -(g_1+g_2)\sum_{j=1}^{m+1} d_j - (g_1I_1 + g_2I_2)$$

If there is no abnormal segments

$$\lambda_N = -(g_1+g_2)l$$

Resistance to flow is given by

$$\lambda_1 = \frac{\lambda}{\lambda_N} = \frac{\sum_{j=1}^{m+1} d_j}{l} + \frac{(g_1I_1+g_2I_2)}{(g_1+g_2)l} \quad (15)$$

Where a stenoses system's walls extend the farthest into the lumen is where the shear stress on those walls is greatest. The point with the highest value of δ_i is referred to as δ_m. After that, using equation (12).

The following expression represents the proportion that lies between the wall shear stress at any given site (τ_R) and the wall shear stress in a normal artery (τ_N).

$$\tau_1 = \frac{\tau_R}{\tau_N} = \frac{g_2 + g_1\left(\frac{R}{R_0}\right)^{-3}}{g_1 + g_2} \tag{16}$$

It is possible to determine the ratio of the maximum wall shear stress to the normal wall shear stress by utilizing the equation (15) and substituting $R = R_0 - \delta_m$. This equation allows us to obtain the ratio.

$$(\tau_1)_{max} = \frac{\tau_R}{\tau_N} = \frac{g_2 + g_1\left(\frac{R_0 - \delta_m}{R_0}\right)^{-3}}{g_1 + g_2} = \frac{g_2 + g_1\left(1 - \frac{\delta_m}{R_0}\right)^{-3}}{g_1 + g_2} \tag{17}$$

For $i = 2$, we get

$$\frac{R}{R_0} = \begin{bmatrix} 1 - B_1\left[l_i^{s_2 - 1}(z - \alpha_2) - (z - \alpha_2)^{s_2}\right] & \alpha_2 \le z \le \beta_2 \\ 1 & Otherwise \end{bmatrix} \tag{18}$$

$$\alpha_2 = \sum_{j=1}^{2}(d_j + l_j) - l_2 = d_1 + l_1 + d_2 + l_2 - l_2 = d_1 + d_2 + l_1 \tag{19}$$

$$\beta_2 = \sum_{j=1}^{2}(d_j + l_j) = d_1 + l_1 + d_2 + l_2 = d_1 + d_2 + l_1 + l_2 \tag{20}$$

$$B_i = \frac{\delta_2}{R_0 l_2^{s_2}} \frac{s_2^{\frac{s_2}{s_2 - 1}}}{s_2 - 1} \tag{21}$$

III. Results and Discussion

Graph I: 3D plot of resistance to flow with stenosis length and dilatation for different values of yield stress

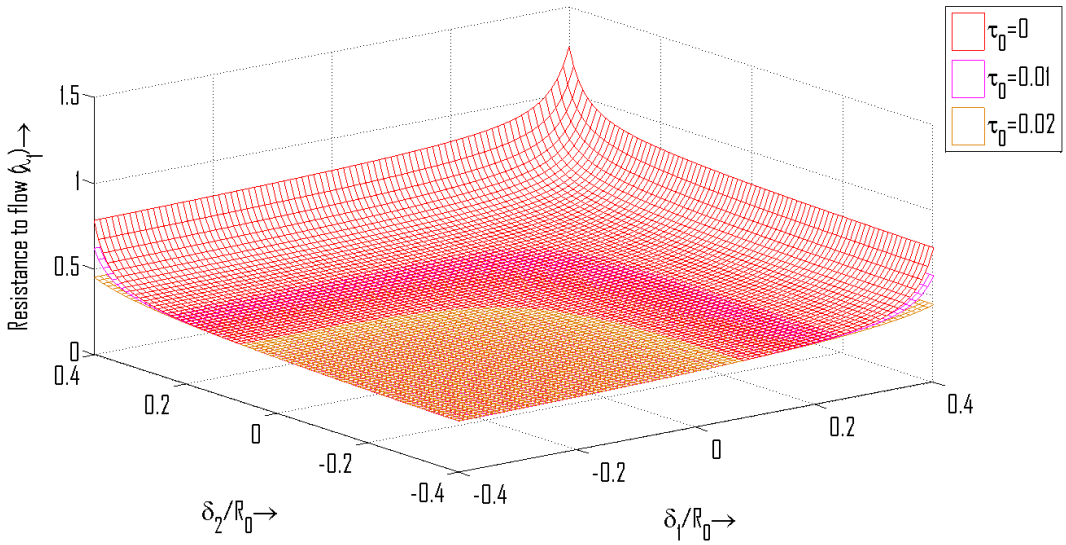

Graph 2: 3D plot of resistance to flow with stenosis length and dilatation for different values of volumetric flow rate

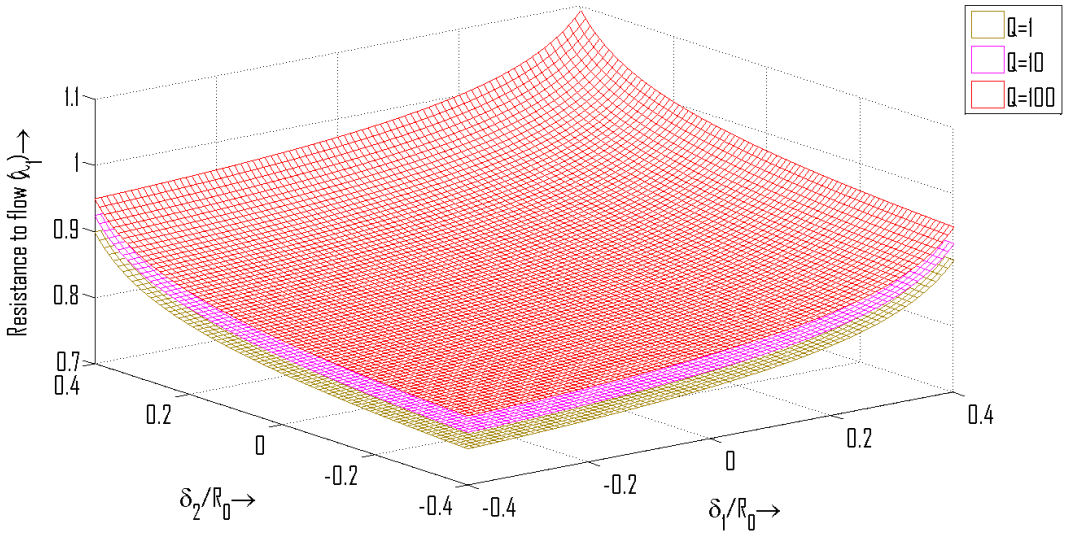

Graph 3: 3D plot of resistance to flow with stenosis length and dilatation for different values of viscosity coefficient

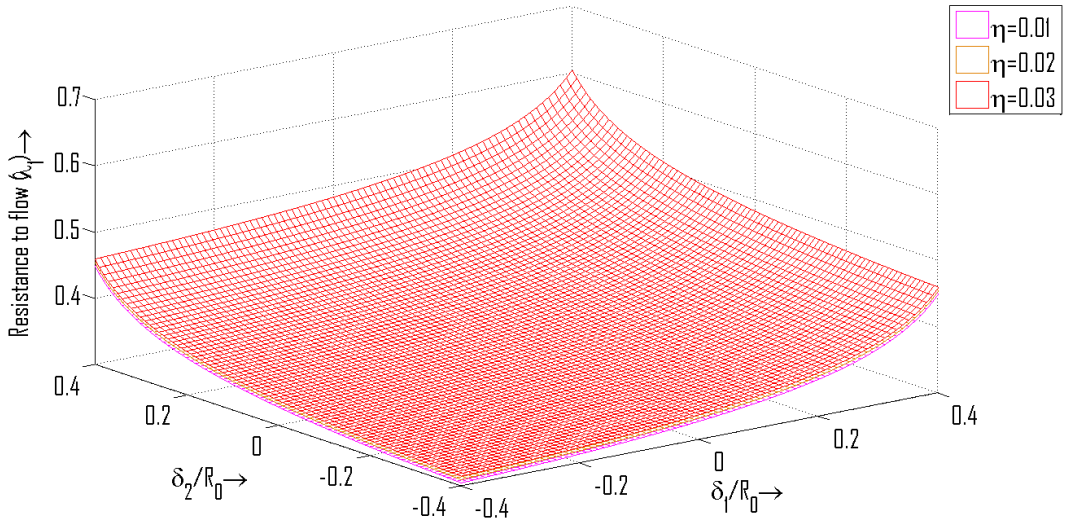

Graph 4:3D plot of resistance to flow with stenosis length and dilatation for different values of shape parameter

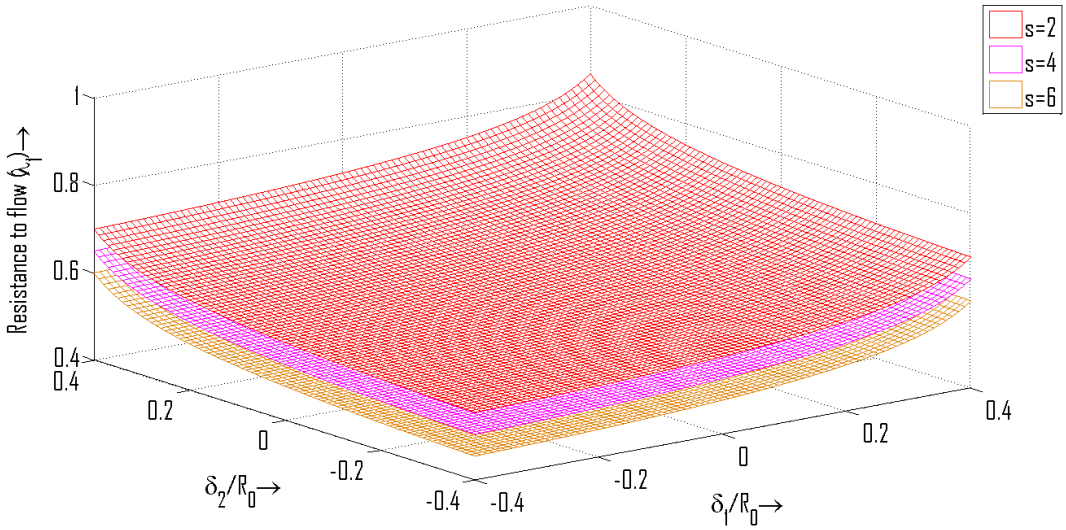

Graph 5: Variation in wall shear stress with aixal distance for different values of yield stress

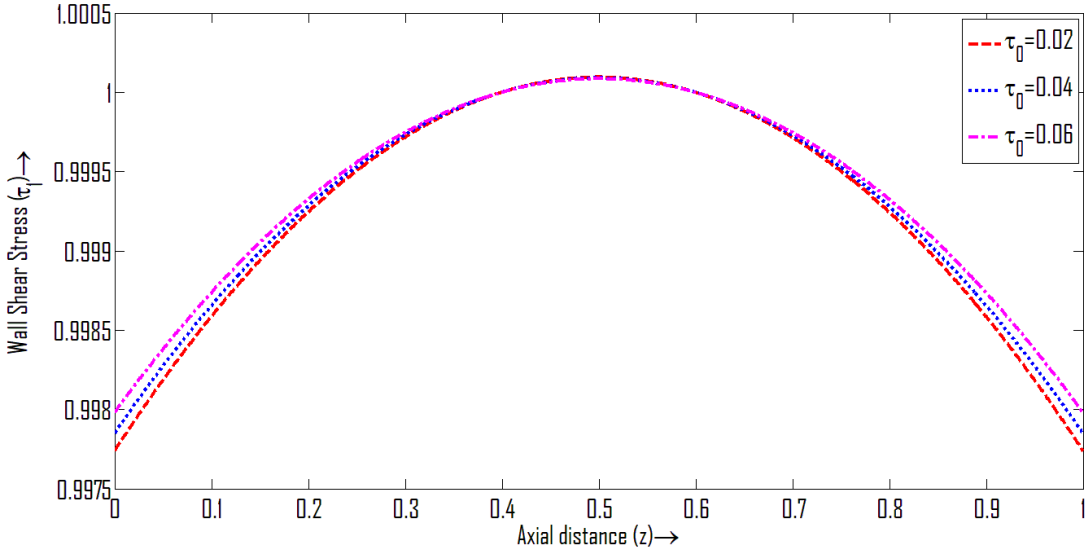

Graph 6: Variation in wall shear stress with aixal distance for different values of dilation heights

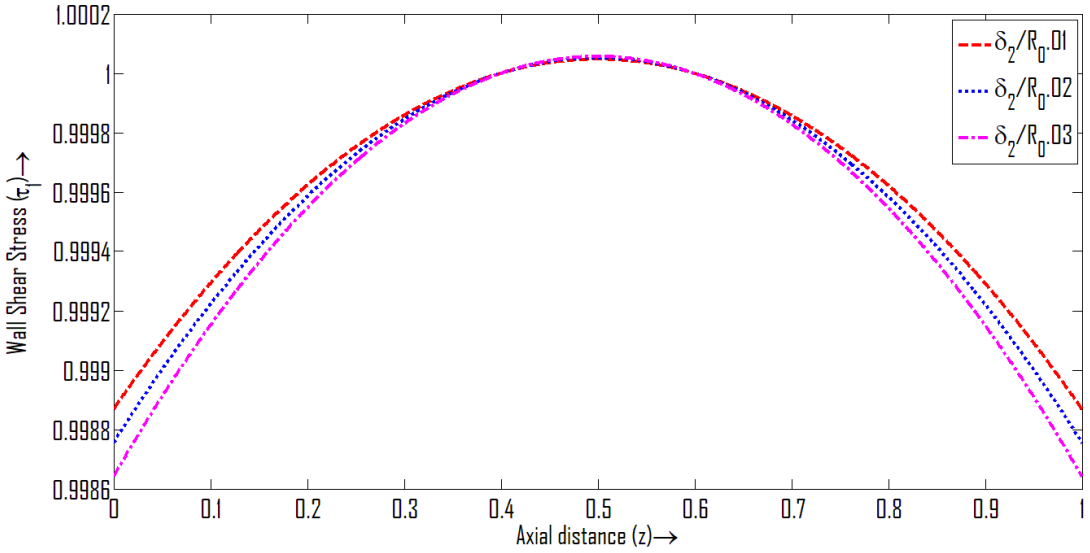

This graph (1) illustrates the three-dimensional change in flow resistance that occurs as a result of stenosis and dilatation length. It also illustrates the various values of yield stress on display. A decrease in flow resistance appears to be a direct consequence of an increase in yield stress, as indicated by the graph. When different amounts of volumetric flow rate are used, the three-dimensional change in flow resistance that is associated with stenosis and dilatation length is depicted in graph (2). This graph reveals that there is a correlation between the increase in volumetric flow rate and the increase in resistance to flow. As the viscosity coefficient is varied, graph (3) shows the three-dimensional fluctuation in flow resistance with respect to stenosis and dilation length. Noticeably, the effect of the viscosity coefficient on flow resistance is somewhat reduced in this graph. The graph (4) illustrates the three-dimensional changes in resistance to flow with regards to stenosis and dilatation length, for various values of the shape parameter. The graph demonstrates that when the form parameter increases, the resistance to flow decreases. For different yield stress values, the variation of wall shear stress with axial distance is shown in graph (5). The graph clearly shows that the wall shear stress grows as the yield stress does. A variety of dilated height values are depicted in graph (6), which shows how the wall shear stress varies with axial distance. It is clear from looking at this graph that the shear force on the wall decreases as the dilated height increases.

IV. Concluding Remarks

Using Ellis fluid biorheology to characterize the hemodynamics of tapering arterial stenosis with dilatation is an important step in understanding the complex dynamics of blood flow in vascular systems. The typical hemodynamic patterns within the circulatory system are greatly disrupted by arterial stenosis, in which blood vessels narrow, and subsequent dilatation, in which arteries widen. Recognizing that blood is not Newtonian and has its own set of rheological characteristics, this study takes a more subtle approach by using Ellis fluid as a model for blood rheology. This study has important implications for clinical practice and the development of therapies to treat vascular diseases because it investigates the hemodynamic complexities of tapered stenosis with dilatation, which improves our knowledge of the complicated fluid dynamics involved. The significance of clarifying the behavior of blood under conditions mimicking tapered arterial stenosis with dilatation is emphasized in this introduction, which sets the stage for a thorough examination of the study's results.

V. Future possibility of Research

There is great potential for future study to further our understanding of vascular pathology through the hemodynamic assessment of tapering arterial stenosis with dilatation employing Ellis fluid biorheology. More complicated depictions of blood flow behavior in such geometries can be obtained by exploring advanced computer modeling techniques, such as fluid-structure interaction models. A combination of patient-specific modeling and integration of in vivo and in vitro experiments can improve

the therapeutic relevance of findings. The construction of tailored treatment plans could be aided by investigating the consequences of various geometric modifications, discovering hemodynamic biomarkers, and performing therapeutic intervention evaluations. Further information on how to improve patient outcomes could be gained from long-term research that investigate the consequences and prognosis of hemodynamic changes in tapering arterial stenosis as dilatation is implemented. Innovative research at the interface of fluid dynamics and biorheology can spark collaborative efforts across disciplines, bringing together cardiology, bioengineering, and biomechanics experts. This research could lead to diagnostic and therapeutic advances.

REFERENCES

1. Chakravarty S., Mandal P.K. (1994): "Mathematical modelling of blood flow through an overlapping arterial stenosis", Mathematical and Computer Modelling, 19 (1):59–70.
2. Chakravarty S., Mandal P.K. (2000): "Two-dimensional blood flow through tapered arteries under stenotic conditions", International Journal of Non-linear Mechanics, 35 (5):779–793.
3. Chaturani P., Ponalagusamy R. (1985): "A study of non-Newtonian aspects of blood flow through stenosed arteries and its applications in arterial diseases", Biorheology 22 (6):521–531.
4. Husaain A., Dar M.N.R., Tag-eldin (2023): "Effects of stenosis and aneurysm on blood flow in stenotic-aneurysmal artery", Heliyon, 9:e17788.
5. Maiti A.K. (2016): "Effect of multiple stenoses and post dilatation on blood flow through an artery", International Journal of Multidisciplinary Research and Development, 3(8):362-366.
6. Oghre E.O., Okoronkwo F.M. (2016): "Bingham fluid model for steady flow in a multi-irregular stenosed artery", Transactions of the Nigerian Association of Mathematical Physics, 2:291-298.
7. Prasad K.M., Sudha T., Phanikumari M.V. (2016): "The effects of post-stenotic dilatations on the flow of couple stress fluid through stenosed arteries", American Journal of Computational Mathematics, 6:365-376.
8. Prasad K.M., Vijaya R.B., Umadevi C. (2014): "Effects of stenosis and post stenotic dilatation on jeffrey fluid flow in arteries", IJRET: International Journal of Research in Engineering and Technology, 4(1): 195-201.
9. Priyadharshini S., Ponalagusamy R. (2015): "Biorheological model on flow of Herschel-Bulkley fluid through a tapered arterial stenosis with dilatation", Applied Bionics and Biomechanics, , Article ID 406195, 12 pages.
10. Raja S.W. , Prasad K.M, Ramana Murthy M.V., Rahim M.A. (2018): "Effect of slip on Herschel- Bulkley fluid flow through an artery with stenosis and post stenotic dilatation", International Journal of Research in Advent Technology, 6(5): 665-670.
11. Singh A.K., Singh D.P. (2012): "A Computational study of Bingham plastic flow of Blood through an artery by multiple stenoses and post dilatation", Advances in Applied Science Research, 3(5):3285-3290.